Maintenance-free Pulse Jet Mixer

ARTICLE *in* POWDER TECHNOLOGY · NOVEMBER 2012

Impact Factor: 2.35 · DOI: 10.1016/j.powtec.2012.07.024

2 AUTHORS, INCLUDING:

Cong Xu
Tsinghua University

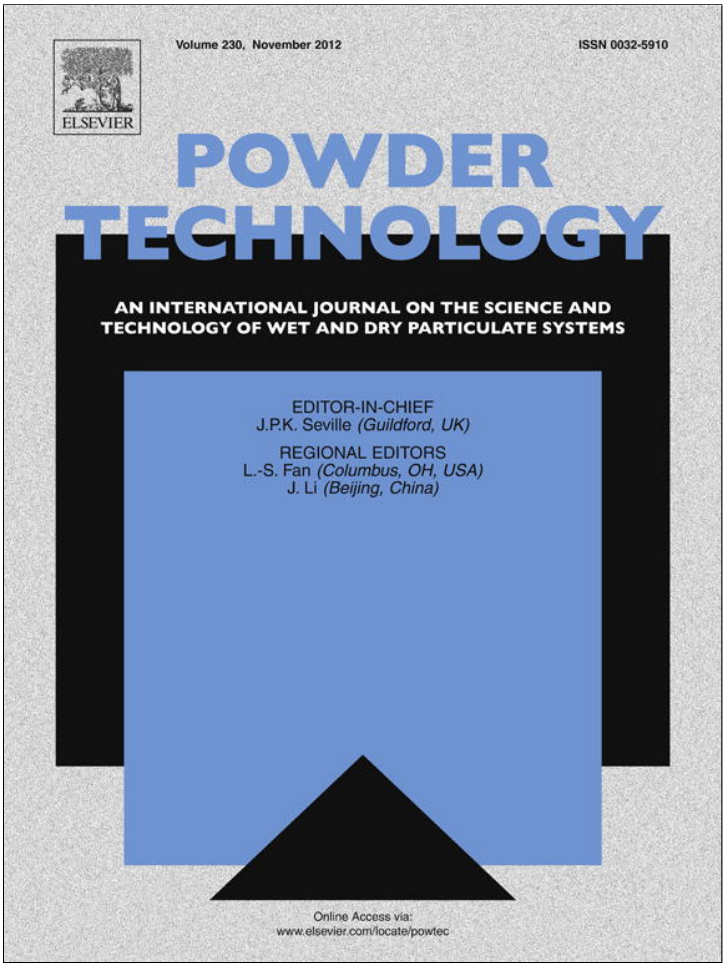
Volume 230, November 2012
ISSN 0032-5910
ELSEVIER
POWDER TECHNOLOGY
AN INTERNATIONAL JOURNAL ON THE SCIENCE AND TECHNOLOGY OF WET AND DRY PARTICULATE SYSTEMS
EDITOR-IN-CHIEF
J.P.K. Seville (Guildford, UK)
REGIONAL EDITORS
L.-S. Fan (Columbus, OH, USA)
J. Li (Beijing, China)
Online Access via:
www.elsevier.com/locate/powtec

Powder Technology 230 (2012) 158–168

Contents lists available at SciVerse ScienceDirect

Powder Technology

journal homepage: www.elsevier.com/locate/powtec

Maintenance-free pulse jet mixer

Cong Xu *, Yi Huang

Institute of Nuclear and New Energy Technology, Tsinghua University, Beijing 100084, PR China

ARTICLE INFO

Article history:
Received 22 July 2011
Received in revised form 5 July 2012
Accepted 7 July 2012
Available online 16 July 2012

Keywords:
Pulse jet mixer
Maintenance-free
Jet pump pair
Vortex diode
Venturi tube
Solid–liquid

ABSTRACT

Maintenance-free pulse jet mixers (PJMs) consisting of a jet pump pair (JPP), gas ballast, and mixing nozzle are applicable for mixing hazardous liquid–solid mixtures that are radioactive, corrosive, and/or toxic. Currently, two problems need to be resolved to realize the potential application of PJMs in hazardous environments. The first problem is the detection of the maximum and minimum fluid levels in the gas ballast, which is independent of any electric components and/or mechanical moving parts directly in contact with a hazardous fluid. The second is how to inhibit the leakage of compressed air during the compression phases of the gas ballast. A novel method for detecting the maximum and minimum fluid levels in the gas ballast was proposed based on the Venturi principle and the sharp variation in the differential pressure signal, respectively. To inhibit the leakage of compressed air, a vortex diode was combined with the JPP, which was proven to be effective. A completely maintenance-free PJM was used to investigate the mixing performance in a water–glycerine–quartz sand mixture. The experimental results showed that the mixing performance improved with increases in the static pressure of the compressed air and the compression time, but decreased with increases in the liquid viscosity and fluid level in the storage tank.

1. Introduction

In the chemical, metallurgical, biological, environmental, and energy industries, considerable amounts of corrosive, toxic, radioactive, or simply high-temperature liquid–solid mixtures are mixed for various purposes. Handling such hazardous fluids poses at least two problems: (1) electric components and mechanical moving parts directly in contact with the fluid are damaged rapidly, and (2) the operation and maintenance staff may be injured. To prevent these problems, remotely controlled maintenance-free mixers having neither electric components nor mechanical moving parts directly in contact with the hazardous fluid are essential. Mixing processes may be classified as mechanical mixing, pneumatic mixing, and jet mixing depending on the mixing power source. Mechanical mixing dependent on stirring paddles is unsuitable in a hazardous environment because of the existence of mechanical moving parts, e.g., a bearing and a rotating shaft. Pneumatic mixing is usually accomplished using gas spargers submerged in the fluid that needs to be mixed. A liquid–solid mixture is mixed by means of the intense turbulence caused by injecting compressed gas into the mixture using the spargers. Because of the lack of mechanical moving parts, pneumatic mixing is more suitable in a hazardous environment than mechanical mixing. However, in practice, one problem restricts the application of pneumatic mixing in processing hazardous mixtures. Although the intense interaction between the gas and the liquid enhances the mixing efficiency, the corrosive, toxic, and/or radioactive elements contained in the mixture may be entrained by the exhaust gas. Therefore, additional exhaust gas treatment is necessary, making the process flow more complex and increasing the costs involved in this process. In contrast to pneumatic mixing, jet mixing [1] is considered more suitable for processing hazardous liquid–solid mixtures because it uses the fluid that needs to be mixed as the working fluid to create a mixing jet flow, which may prevent the production of a large amount of exhaust gas. In recent years, several studies on jet mixing have been reported. Kalaichelvi et al. [2] and Patwardhan et al. [3] investigated the effects of exit diameter, tilt angle and layout of mixing nozzles, and jet velocity on the mixing time. Patwardhan et al. [4,5] used computational fluid dynamic simulations to confirm that the mixing time decreases with an increase in the exit diameter of the mixing nozzle. Zughbi et al. [6,7] also investigated the effects of the number, layout, and tilt angle of mixing nozzles via computational fluid dynamic simulations. In these studies, the jet flow was usually created using a mechanical device, e.g., a centrifugal pump, which is unsuitable for mixing hazardous fluids. A novel jet mixer known as a pulse jet mixer (PJM) can be fabricated by replacing the conventional mechanical pump with a gas ballast, which contains no mechanical moving parts. The PJM is designed for mixing hazardous fluids, e.g., radioactive sludge.

A PJM consisting of a jet pump pair (JPP), gas ballast, and mixing nozzles is a completely gas-motivated mixing system. The liquid–solid mixture that needs to be mixed is discharged and drawn into the gas ballast periodically by alternating the gas ballast between the compression and suction phases. In the compression phase, the compressed gas forces the mixture drawn into the gas ballast to be ejected from the mixing nozzle connected to the bottom of the gas ballast. Unlike a

* Corresponding author. Tel.: +86 10 89796075; fax: +86 10 62771740.
E-mail address: c-xu@mail.tsinghua.edu.cn (C. Xu).

0032-5910/$ – see front matter © 2012 Elsevier B.V. All rights reserved.
doi:10.1016/j.powtec.2012.07.024

pneumatic mixer, gas contact exists only with the fluid (hazardous liquid–solid mixture) surface in the gas ballast. Thus, none or few of the hazardous elements may be entrained by the exhaust gas. In the 1990s, PJMs were studied for implementation in waste disposal plants in the USA [8]. The Oak Ridge National Laboratory, USA, further investigated the mixing performance of a PJM developed in Russia for radioactive sludge in 2001, in which the compression pressure reached 1206 kPa [9]. In 2003, the Hanford radioactive waste disposal site in the USA tested PJMs with different dimensions and layouts [10]. To determine the optimum conditions for mixing, Guerrero et al. [11] investigated the effects of the nozzle exit diameter, jet velocity, circulating time of pulse jet flow, and layout of mixing nozzles. On the basis of experimental results, Bamberger et al. [12] established a relationship among jet velocity, mixing time, and particle concentration. Moreover, Rosendall et al. [13] simulated the mixing performance of a PJM used for radioactive liquid waste and compared the simulated results with those of experiments. The results for the area close to the bottom of the tank were very consistent, but there was an obvious deviation for the area far away from the bottom of the tank.

Although numerous studies on PJMs have been conducted in the past decade, in practice, two problems still remain that reduce the potential use of PJMs in hazardous environments. The first is how to detect the maximum and minimum fluid levels in the gas ballast. Conventional direct-contact fluid level detectors, e.g., capacitive, electroconductive, and radio-frequency level detectors, are unsuitable because of their electric components and mechanical moving parts, which would be in direct contact with the hazardous fluid. Indirect-contact level detectors, e.g., radar and supersonic level detectors, are also unsuitable for detecting the level change of a hazardous fluid in a gas ballast. This is because it is very difficult to keep the detector probe constantly perpendicular to the fluid surface, which fluctuates during the operating cycle of the gas ballast. In addition, to prevent excessive fading of the measurement wave when a supersonic wave passes through the ballast wall, indirect-contact level detectors must be set up inside the gas ballast. Accordingly, the electric components in the detectors are easily damaged by the hazardous atmosphere, which results in frequent maintenance. The second problem is how to inhibit the leakage of compressed gas during the compression phase of the gas ballast. The leakage of the compressed gas decreases the energy conversion efficiency significantly. To date, these two problems have not been resolved. Moreover, the experiments investigating a PJM's mixing performance have been insufficient because it is difficult to measure the local solid concentration in real time. Hence, this study focuses on these problems.

2. Experimental

2.1. PJM and working processes

Fig. 1 shows a flow chart of a maintenance-free pulse jet mixing system, which consists mainly of a JPP, gas ballast (including mixing nozzles), and fluid level detectors.

1—Gas ballast; 2—Venturi tube; 3—vortex diode; 4—piezometric tube at minimum level; 5—mixing nozzle; 6—JPP; 7—differential pressure transducer; 8—analog-to-digital converter; 9—computer; 10—digital-to-analog converter; 11—compression electromagnetic valve; 12—suction electromagnetic valve; 13—pressure surge tank; 14—compressor; 15—flowmeter; 16—pressure transducer; 17—storage

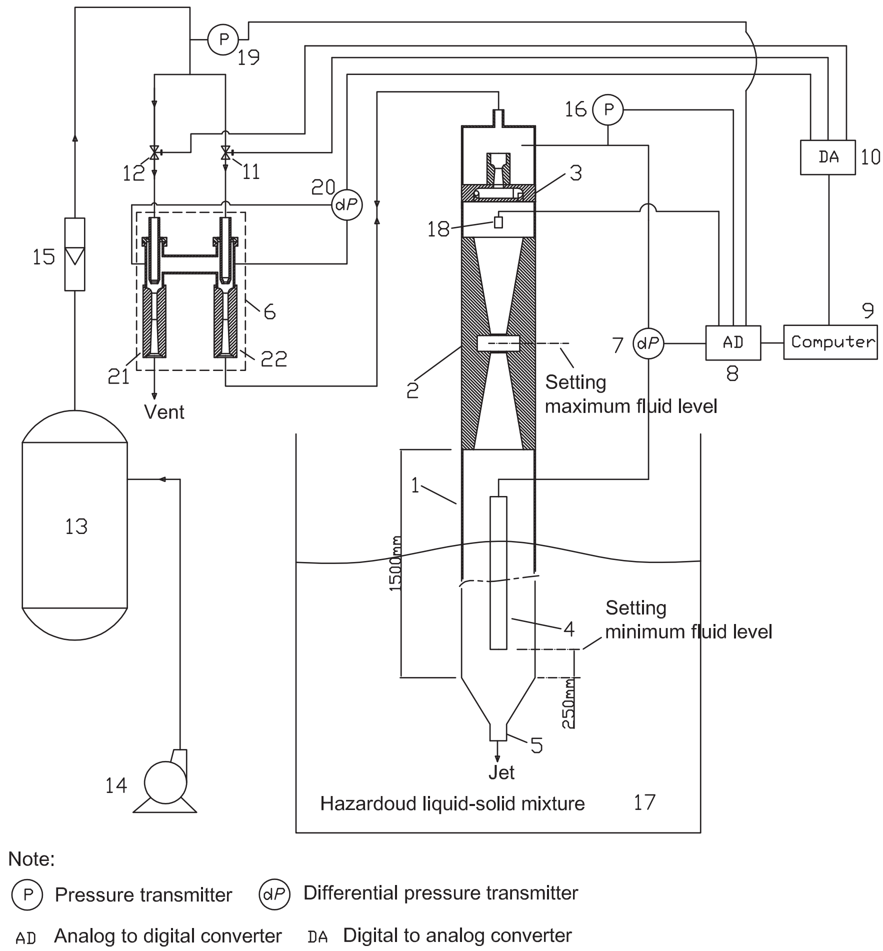

Fig. 1. Schematic of the maintenance-free pulse jet mixing system.

tank; 18—ultrasound level meter; 19—pressure transducer; 20—differential pressure transducer; 21—suction injector; 22—compression injector.

The configuration of the PJM adopted in this study is shown in Fig. 2. A stainless steel barrel with an inner diameter of 0.1 m and a length of 1.5 m was used as the gas ballast; a replaceable section was screwed onto the bottom of the barrel. In this replaceable section, a mixing nozzle was connected to the vertical barrel wall through a conical section. The JPP shown in Fig. 3 was used to supply compressed air and vacuum for the compression phase and suction phase of the gas ballast, respectively. The JPP consisted of two air injectors, the compression injector and the suction injector, connected by a tube. Each injector consisted of an air jet nozzle, throat tube, and diffuser. The diffuser exit in the compression injector was connected to the gas ballast via a pipe. The compression and suction injectors were both connected to a pressure surge tank, and two electromagnetic valves were set up in the inlet pipes. The pressure/differential pressure, fluid level in the gas ballast, and local particle concentration in the storage tank were determined in real time using pressure/differential pressure transducers, a supersonic fluid level detector, and a fiber-optic apparatus for measuring particle concentration, respectively. The PJM working process can be divided into three phases as follows.

- Suction phase (Fig. 4-a): The suction electromagnetic valve opens and compressed air is ejected from the nozzle exit in the suction injector, creating an air jet flow across the throat tube. Therefore, a low-pressure area surrounding the jet core is formed, and the gas in the ballast is exhausted through the compression diffuser–connection tube–suction diffuser. Subsequently, the mixture in the

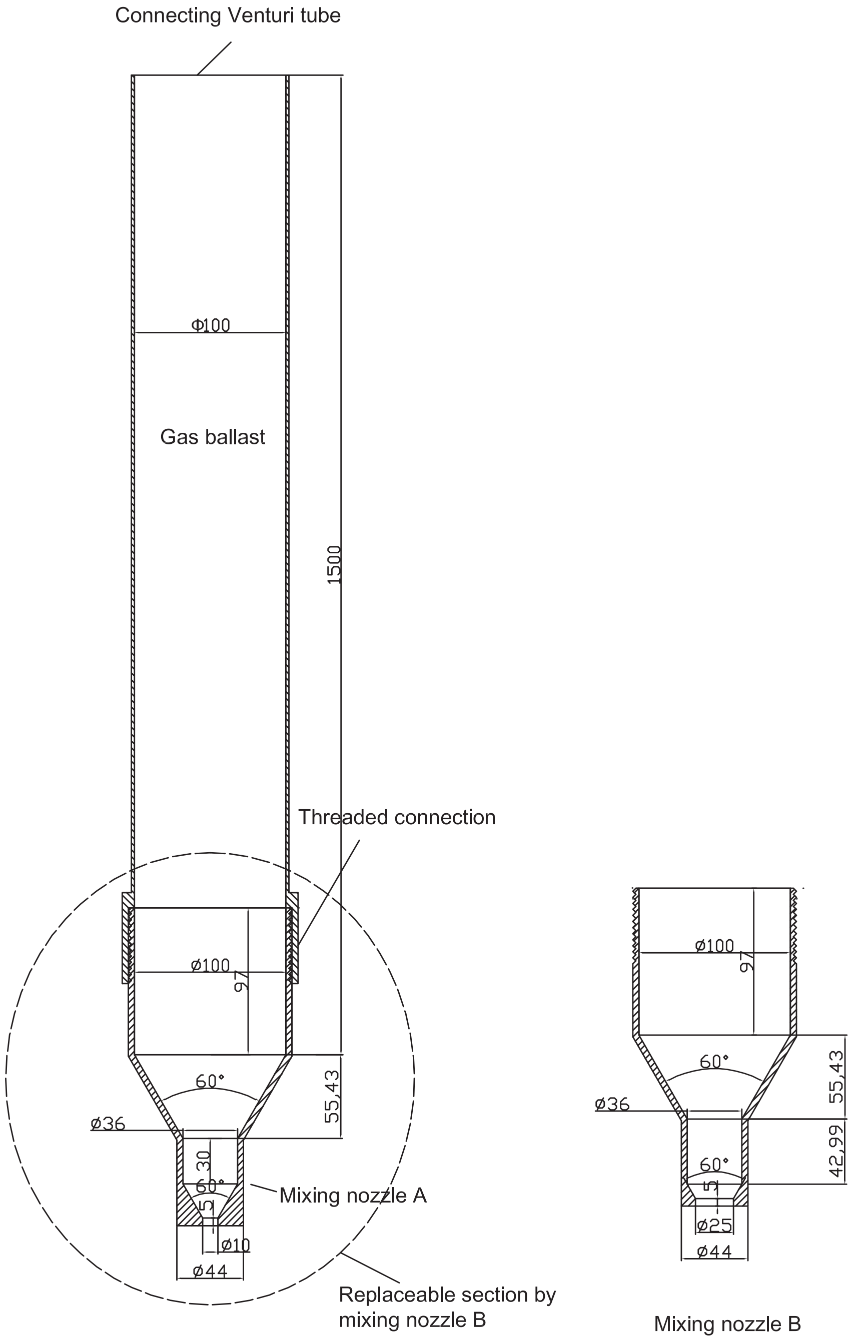

Fig. 2. Geometric configuration of PJM.

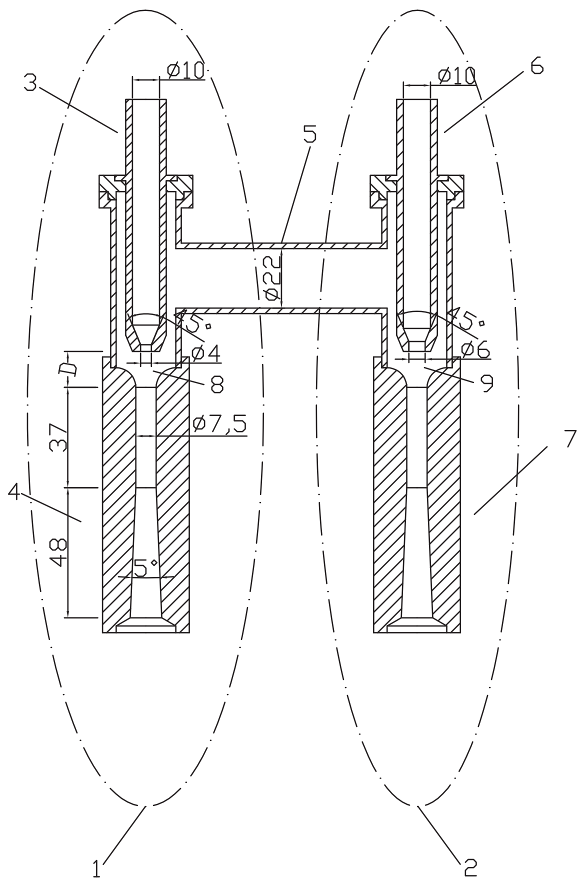

Fig. 3. Geometric configuration of JPP.

storage tank is drawn into the gas ballast until it is full (reaching the maximum-level setting).

- Compression phase (Fig. 4-b): When the ballast is filled with the mixture, the compression electromagnetic valve opens and the suction electromagnetic valve closes. The compressed air ejected from the compression nozzle acts on the mixture in the ballast through the compression diffuser. The compressed air forces the mixture to be ejected from the mixing nozzle connected to the ballast and creates a mixing jet in the storage tank. Because of the shearing action caused by this mixing jet, numerous vortexes are formed, inducing an ambient fluid into the mixing jet where they exchange energy and momentum. Moreover, the fluid adjacent to the mixing nozzle may generally be circulated over a specific bulk volume of the tank (bulk-flow). Therefore, the fluids in the tank are mixed under the influence of the shearing action and bulk-flow. As the fluid level in the ballast drops to the minimum-level setting, the compression electromagnetic valve closes and the compression phase is finished.
- Vent phase (Fig. 4-c): Both the suction and the compression electromagnetic valves are closed for a set time t_v, and the compressed air remaining in the ballast is exhausted through the compression diffuser–connection tube–suction diffuser. During this phase, the pressure in the ballast is reduced to environmental pressure. Once the vent phase is completed, the suction electromagnetic valve is opened again and the PJM initiates the suction phase. The PJM is operated repeatedly in a suction–compression–vent cycle to mix the liquid–solid mixture in the tank.

During the operating cycle, the pressure in the gas ballast varies similar to a pulse. As mentioned above, it is obvious that (1) the compressed air is used to force the fluid flow, (2) the fluid that needs to be mixed is used to create the mixing jet in the storage tank, (3) the switch between working processes is dependent on the JPP without any mechanical moving parts, and (4) the gas ballast also contains no mechanical moving parts in direct contact with the fluid that needs to be mixed. Hence, the PJM is very suitable for mixing toxic, corrosive, radioactive, high-temperature, and/or high-solid-content hazardous liquid–solid mixtures.

1—Suction injector; 2—compression injector; 3—suction nozzle; 4—suction diffuser; 5—connection tube; 6—compression nozzle; 7—compression diffuser (identical to suction diffuser); 8—suction throat; 9—compression throat.

2.2. Measuring apparatus

As illustrated in Fig. 1, the pressure data in the suction injector inlet (P_j), compression injector inlet (P_h), and compression diffuser outlet (P_d) were acquired in real time using SY-9411 pressure transmitters (Beijing ShengYe Co., Ltd., span 500 kPa, accuracy $\pm$0.5%). Differential pressure data between the ends of the connection tube in the JPP and between the upper and lower sides of the Venturi tube (illustrated in detail in Section 3.1) were measured using two CECC-430G capacitive differential pressure meters (Shanghai GuangHua Instrument Co., Ltd., span 10 kPa, accuracy 0.5%). The viscosity and density of the liquid phase for the liquid–solid mixture were determined using a DV-1 rotary viscosimeter (Spain FUNGILAB Co.) and a Den Di-1 density meter (China Beijing YILUDA Co., Ltd.), respectively. The particle diameter distribution for the solid phase was determined using a Mastersizer 2000 particle size distribution analyzer (U.K. Malvern Instruments Co., Ltd.). A supersonic fluid level meter (RPS-426A-80, U.S. MIGATRON Co.) was installed on the top of the ballast to measure the variation in the fluid level in the ballast during the operating cycle. The supersonic fluid level meter was calibrated in a transparent Plexiglas gas ballast. The local solid concentrations in different regions of the tank were acquired using a fiber-optic particle concentration meter having eight channels (PC-8, Institute of Process Engineering, Chinese Academy of Sciences) to evaluate the mixing performance of the PJM.

2.3. Liquid–solid mixture

The liquid–solid mixture adopted in this study was prepared using water, glycerine, and quartz sand; the glycerine was used to regulate the viscosity of the liquid phases. The material properties are as follows:

Glycerine: purity, 99.7%; melting point, 18.17 °C; density, 1.261 g/cm^3 (25 °C); dynamic viscosity, 9.54 Pa·s (25 °C).
Quartz sand: $SiO_2 \geq$ 90%–99%; $Fe_2O_3 \leq$ 0.06%–0.02%; density, 2.65 g/cm^3 (25 °C). The particle size distribution is shown in Fig. 5.

The physical properties of the quartz–glycerine–water mixture are listed in Table 1.

3. Results and discussion

3.1. Method for detecting maximum and minimum fluid levels in the gas ballast

A novel, maintenance-free fluid level detection system (Fig. 1) was proposed. It contained four parts: a piezometric tube whose open end flushes at the minimum-level setting, Venturi tube located in the upper section of the ballast, vortex diode over the Venturi tube, and differential pressure meter. The piezometric tube was a stainless steel barrel with an inner diameter of 20 mm and a length of 1200 mm. A stainless steel pipe with an inner diameter of 4 mm was set up to connect the top of the piezometric tube to the high-pressure hole of the differential pressure meter. In the Venturi tube, a convergent nozzle was coaxially mounted opposite to a divergent diffuser and a chamber

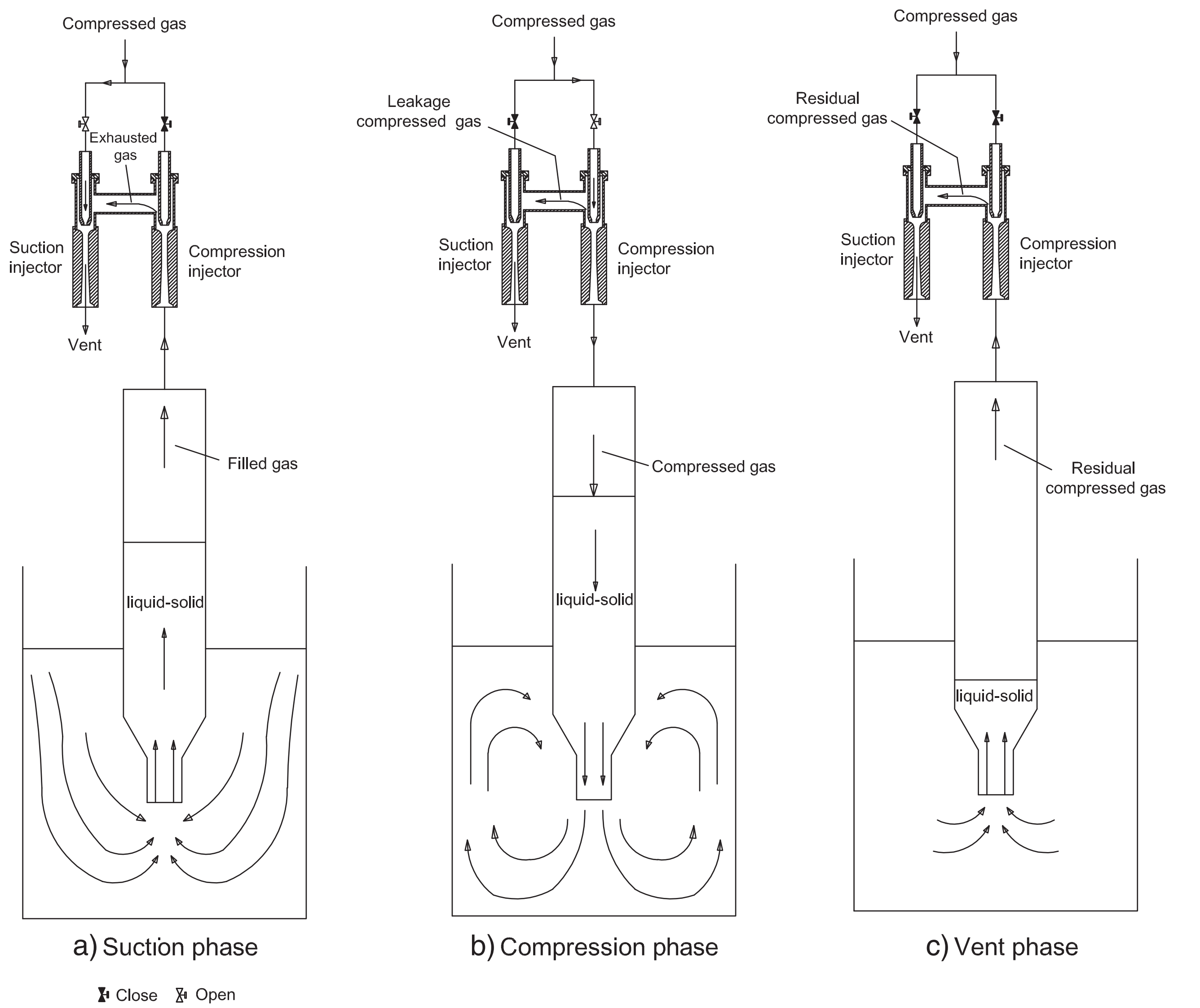

Fig. 4. Working processes of PJM.

separated the two (Fig. 6). The horizontal centerline of the chamber was flushed with the maximum-level setting. A vortex diode is a novel fluidic component similar to a flat disc chamber with an axial port and four tangential ports (Fig. 7). A stainless steel pipe with an inner diameter of 4 mm was connected to the low-pressure hole of the differential pressure meter and was placed above the vortex

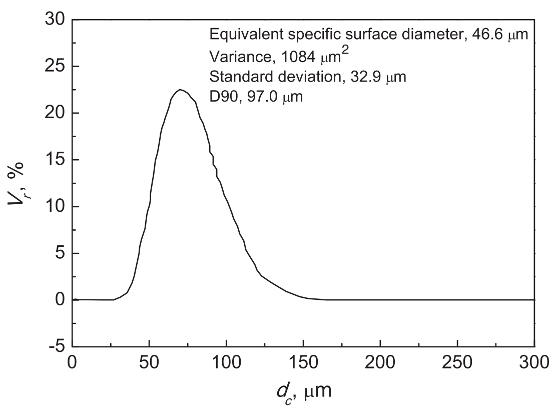

Fig. 5. Particle size distribution of quartz sand.

diode. The working principle of the fluid level detection system is as follows:

- Maximum-level detection (suction phase, S stage in Fig. 8): The mixture in the tank is drawn into the ballast, which produces a rapid rise in the fluid level during the suction phase of the PJM. When the fluid level passes the open end (minimum-level setting) at the bottom of the piezometric tube, a rising fluid column is formed in the piezometric tube. This fluid column rises continually with the fluid level in the ballast and compresses the remaining air at the top of the piezometric tube. Consequently, the differential pressure meter generates a continuously increasing signal (dP_V), except at the beginning stage when the open end is not immersed in the fluid. An important trend should be addressed for the increasing signal. Only air passes through the Venturi tube because the mixture does not enter this tube. Consequently, in this stage, the energy loss attributed to flow friction of air is lower and may be characterized using the differential pressure dP_V. When the liquid–solid mixture enters the Venturi tube and flows past the chamber between the nozzle and diffuser, dP_V increases suddenly because of the greater energy loss than that caused by air flow. A sudden increase in the slope coefficient of the dP_V–time curve should appear as the liquid–solid mixture flows through the chamber. Maximum-level

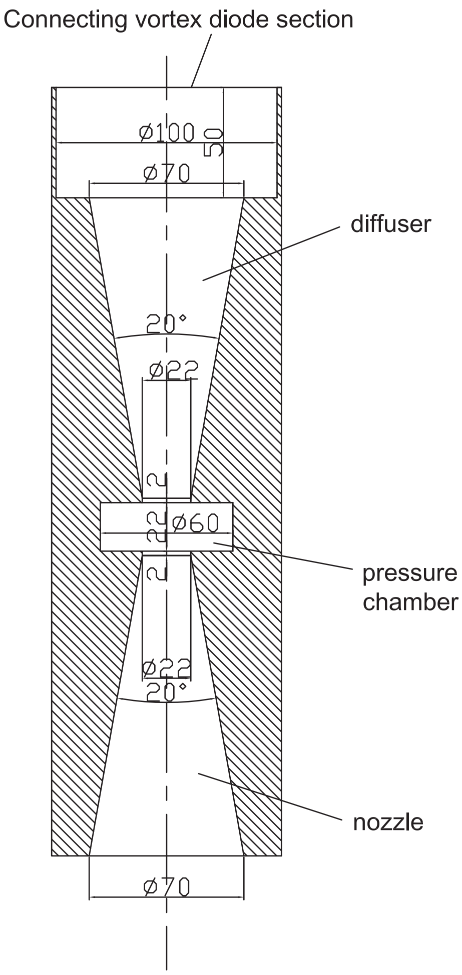

Fig. 6. Venturi tube for maximum-level detection in the gas ballast.

detection may thus be achieved on the basis of this phenomenon. To prevent the rising mixture from rushing into the compression/suction pipe above the ballast, which would result in the diffusion of radioactivity, corrosivity, or toxicity, a vortex diode is installed over the Venturi tube. As illustrated in Fig. 9, when the liquid–solid mixture enters the disc chamber from tangential ports, it should form a vortex flow surrounding the axial port because of the high tangential flow velocity, which produces a high flow resistance area around the axial port. This area may inhibit the liquid–solid mixture from discharging out of the axial port and then entering the compression/suction pipe.

- Minimum-level detection (compression, C stage in Fig. 8): In contrast to the suction phase, compressed air enters the disc chamber through the axial port during the compression phase. As illustrated in Fig. 9, this compressed air further enters the volume of the ballast under the vortex diode along the radial direction of the disc chamber and through the tangential ports. In comparison with the vortex flow of the liquid–solid mixture from the tangential ports to the axial port, the flow resistance of the air from the axial port to the tangential ports is lower. Compressed air discharging out of the tangential ports acts on the liquid–solid mixture, forcing the mixture to be ejected from the mixing nozzle located at the bottom of the ballast and creating a mixing jet flow in the tank. During this phase, the fluid column in the piezometric tube falls with the declining fluid level in the ballast, causing a decrease in gas pressure at the top of the piezometric tube. Because of the comparatively constant pressure inside the ballast under the vortex diode, the differential pressure meter should generate a negative dP_v, which decreases continually with the declining fluid level. When the declining fluid level goes below the open end of the piezometric tube (minimum-level setting), the fluid column rapidly drains into the ballast from the piezometric tube under gravity. At this time, the differential pressure meter generates a V-shaped variation from a negative value to the zero point in the dP_v–time curve. It should be noted that the V-shaped variation in the dP_v signal appears only because the fluid level is below the open end of the piezometric tube during the compression phase. Minimum-level detection can thus be dependent on this phenomenon.

Table 1
Parameters of solid–liquid mixtures prepared in experiments.

Number	Mass percent of glycerine (%)	Mass percent of quartz sand (%)	Liquid phase viscosity (mPa·s)	Liquid phase density (g/cm3)
1	0	0	1.21	0.9992
2	0	36.31	1.21	0.9992
3	20	36.31	3.76	1.2003
4	40	36.31	8.39	1.2119
5	60	36.31	23.69	1.2337

As mentioned above, the proposed maximum/minimum fluid level detection system has no mechanical moving parts directly in contact with the liquid–solid mixture. In addition, electrical components such as the differential pressure meter can be installed in an area beyond the hazardous storage tank.

A part of the dP_v–time curve is shown in Fig. 8 under the conditions that the static pressure of the compressed air is 160 kPa (gauge) and the period of the vent phase is 25 s. In this test, at least 100 cycles (suction–compression–vent) were performed depending on the level detection system; in this system, no liquid–solid mixture was drawn into the compression/suction pipe above the ballast during the suction phases and no compressed air was injected into the tank through the mixing nozzle during the compression phases.

3.2. Inhibition of leakage of compressed gas during the compression phase

Ideally, all the compressed air ejected from the compression nozzle is injected into the ballast to force the fluid to create a mixing jet in the tank. However, in practice, a large part of the compressed air cannot enter the compression diffuser and move into the ballast. Instead, it is discharged from the suction diffuser exit through the connection tube, which results in a serious energy loss and reduces the mixing efficiency of the PJM. This is a persistent problem that needs to be resolved in order to realize the potential use of PJMs. The key to resolving the problem is determining how to inhibit the leakage of compressed air from the compression nozzle exit to the suction diffuser without mechanical moving parts. A novel fluidic component, the vortex diode, was employed in this study to inhibit the leakage of compressed air without excessively affecting the performance of the suction injector.

3.2.1. Design for inhibiting leakage

The configurations and sizes of the vortex diodes designed for inhibiting the leakage of compressed air are illustrated in Fig. 10. As shown in Fig. 11, the connection tube is split, and one branch close to the suction injector is connected to the axial port of the vortex diode and the other is connected to the tangential port of the vortex diode. The principle for inhibiting the leakage of compressed air during the compression phase is identical to the principle for restricting gas flow from the tangential port to the axial port (Fig. 9). It should be noted that the vortex flow resistance is dependent on the tangential flow velocity of the gas entering the disc chamber, with a higher tangential flow velocity producing a greater vortex flow resistance.

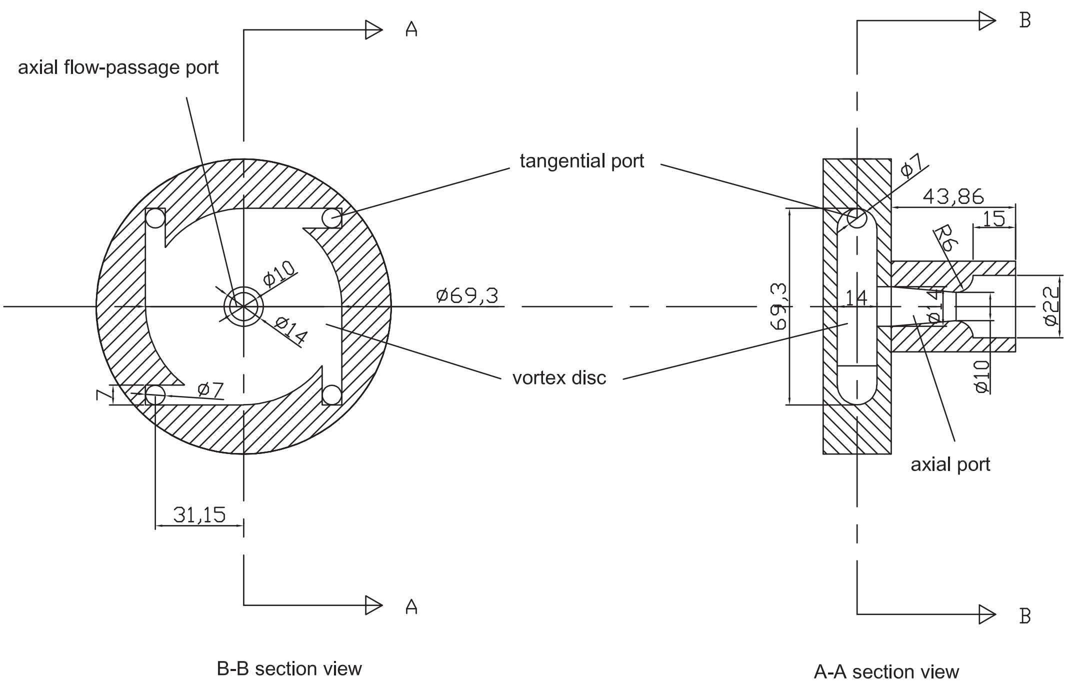

Fig. 7. Vortex diode used to prevent fluid from overflowing out of the gas ballast.

Using this vortex flow feature, we can achieve gas flow from the tangential port to the axial port during the suction phase with a lower resistance than that during the compression phase. This is because the gas flow from the tangential port to the axial port during the suction phase is driven by the jet entrainment action in the suction injector, whereas that during the compression phase is caused by the large volume of high-pressure compressed air that flows directly into the tangential port. Hence, the tangential velocity during the suction phase is lower than that during the compression phase. As a result, although the flow resistance during the suction phase with a vortex diode is slightly higher than that without the vortex diode, the inhibition of the leakage of compressed air with the vortex diode is more obvious during the compression phase. Therefore, the overall performance of the JPP with a vortex diode is effectively improved.

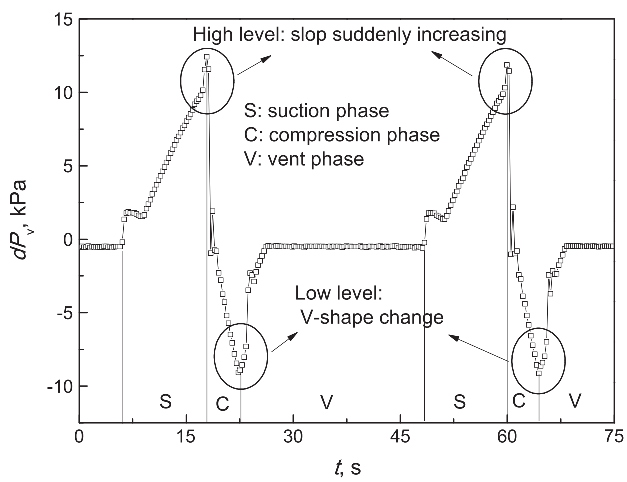

Fig. 8. Pressure difference data dP_v acquired in real time (mixing nozzle B; d_1, 4 mm; d_2, 6 mm; D, 17.25 mm; H_b, 10 cm; H_l, 120 cm; H_v, 5 0 cm).

3.2.2. Effects of vortex diode on inhibition of leakage of compressed gas

The following parameter was defined to evaluate the effective inhibition of the leakage of compressed air:

$$\lambda = dP_{c,j}/dP_{s,j} \tag{1}$$

where $dP_{c,j}$ and $dP_{s,j}$ denote the differential pressures between the connection tubes during the compression phase and the suction phase, respectively. The parameter characterizes the extent of leakage during the compression phase because the suction injector performance during the suction phase is almost invariable. A smaller value of the parameter indicates better inhibition of leakage of compressed gas during the compression phase. Fig. 12 shows the results with and without the vortex diode. Obviously, λ is lower with the vortex diode than without it, and the extent of its reduction is about 50%.

The experimental results for the jet flow velocity at the mixing nozzle exit during the compression phase are shown in Fig. 13. These results were calculated using the data for the fluid level in the ballast measured by the supersonic level meter. The mixing jet flow velocity with the vortex diode is evidently greater than that without it when the static pressure of the compressed air is constant. Therefore, the vortex diode efficiently inhibits the leakage of compressed air during the compression phase.

3.3. Mixing performance

A complete maintenance-free PJM was investigated in this study to evaluate its mixing performance for a liquid–solid mixture, where mixing nozzle A was adopted. The storage tank was a stainless steel drum with a 120-cm inner diameter. The axial centerline of the PJM was coincident with that of the drum. Given that the fluid flow in the tank was axially symmetrical, the fiber-optic probes used to measure the local particle concentration were arranged as illustrated in Fig. 14. The detailed layout parameters are listed in Table 2.

Before the mixing tests, all the optic probes were calibrated using a uniform liquid–solid mixture with a known particle concentration.

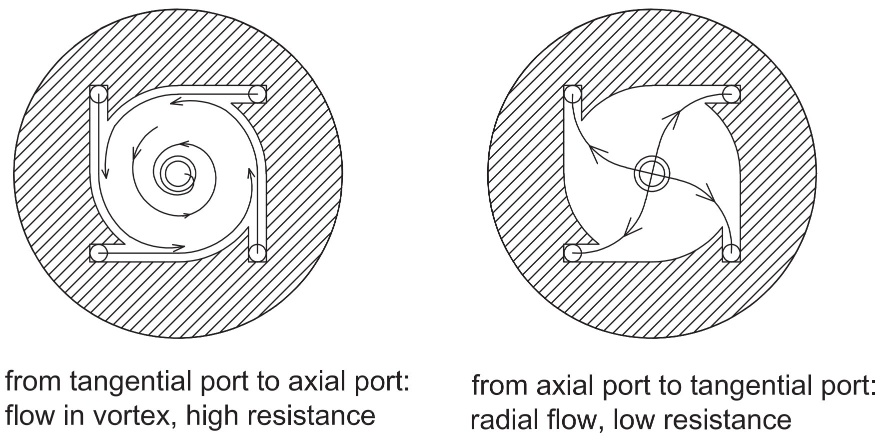

Fig. 9. Working principle of vortex diode.

In the mixing process, the local particle concentrations at different locations were determined using a particle concentration meter. A parameter η is defined as the average mixing index for evaluating the mixing performance of the PJM and is expressed as follows.

$$\eta = \frac{\sum_{i=1}^{n} \left| \frac{c_i - c_{i0}}{\bar{c} - c_{i0}} \right|}{n} \tag{2}$$

where c_{i0} denotes the volume concentration of the particles at location i before the mixing process starts; c_i, the time-averaged volume concentration of the particles at location i as the mixing process becomes stable (a stable mixing state is described in Section 3.3.1); and $\bar{c}$ $(=V_s/(V_s+V_l))$, the ideal volume concentration of the particles over the entire tank as the liquid–solid mixture is uniformly mixed. η denotes the extent of mixing of the liquid–solid mixture over the volume framed by the optic probes ($n=16$). A higher η indicates more intense mixing between the liquid and solid phases. Therefore, the mixing efficiency is excellent.

3.3.1. Effects of static pressure of compressed air

Compressed air is the power source of the mixing process. As the static pressure of the compressed air increases, an intense mixing jet can be formed under the impelling action of the compressed air. The effects of the static pressure on the mixing performance of the PJM were examined under the following conditions: exit diameter of the suction nozzle, $d_1=4$ mm; exit diameter of the compression nozzle, $d_2=6$ mm; suction throat length, $D=17.25$ mm; exit diameter of mixing nozzle A, $d_g=10$ mm; mass concentration of particles = 36.31%; initial height of the solid layer = 10 cm; liquid viscosity, $\mu=1.21$ mPa·s; height of the mixing nozzle exit from the tank bottom, $H_b=10$ cm; maximum-level setting in the ballast, $H_1=120$ cm; height of the fluid level in the tank, $H_v=30$ cm; and vent period, $t_1=10$ s.

Fig. 15 shows the experimental results. The mixing index η clearly increased with an increase in the static pressure. Increasing the mixing jet flow velocity with increasing static pressure can efficiently enhance the mixing performance of the PJM because of more intense turbulence and circulating bulk-flow.

Fig. 16 presents the results of local particle concentration at location 3, as illustrated in Fig. 14, with time. The local particle concentration is found to be periodic after a certain time δt. This phenomenon indicates that the PJM mixing cycle no longer improves the mixing of the liquid–solid mixture when it exceeds δt. We define δt as the stable mixing time at location 3, which indicates that the local particle concentrations become constant or periodic after the PJM mixing cycle continues to run after δt. Evidently, a smaller stable mixing time represents a PJM having a better mixing performance. For convenience, all the following experiments use the stable mixing time at location 3 to evaluate the mixing performance of the PJM. As shown in Fig. 17, the stable mixing time at location 3 also decreases with increasing static pressure of the compressed air. Thus, a higher static pressure was proven to be beneficial for enhancing the mixing performance of the PJM.

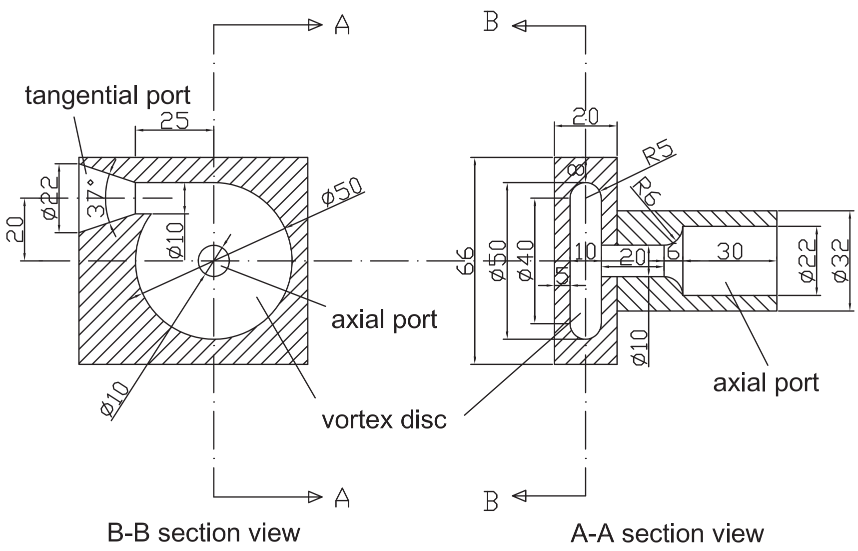

Fig. 10. Configuration of the vortex diode used to inhibit the leakage of compressed gas during the compression phase.

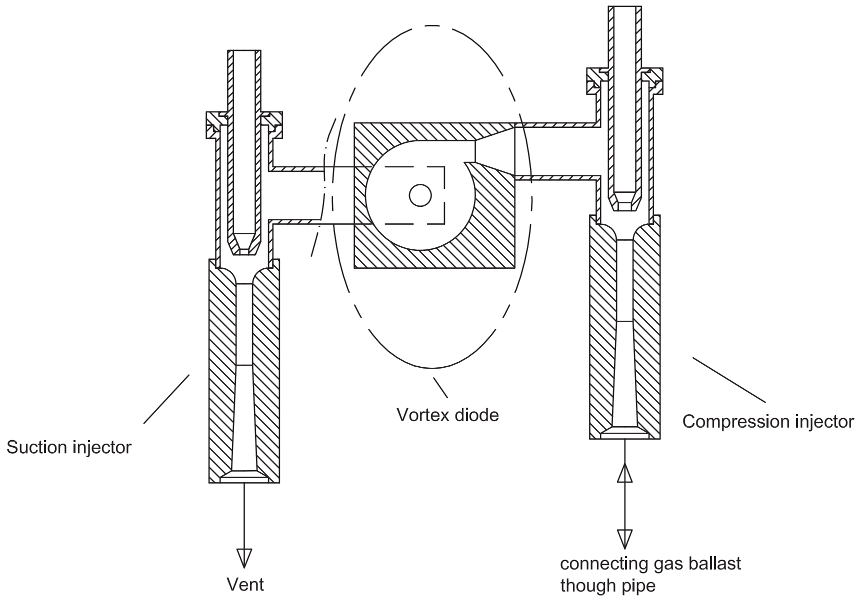

Fig. 11. Layout of JPP with a vortex diode.

3.3.2. Effects of liquid viscosity

The shear force on the liquid–solid interface is directly governed by the liquid viscosity, which is a key factor influencing the mixing performance of the PJM. The effects of the liquid viscosity on the mixing performance of the PJM were examined under the following conditions: mass concentration of the particles = 36.31%; initial height of the solid layer = 10 cm; height of the mixing nozzle exit from the tank bottom, $H_b = 10$ cm; maximum-level setting in the ballast, $H_1 = 120$ cm; height of the fluid level in the tank, $H_v = 30$ cm; static pressure of the compressed air, $P_{c0} = 260$ kPa; and vent period, $t_1 = 10$ s.

As shown in Fig. 18, the average mixing index η decreases with an increase in the liquid viscosity. When the liquid viscosity is high enough, η may even be close to zero, indicating that the local solid layer is not mixed by the PJM. Because of the increasing viscous force, the mixing jet flow velocity obviously decreases with increasing liquid viscosity during the compression phase. The turbulence and circulating bulk-flow caused by the mixing jet decrease with an increase in liquid viscosity, which results in a low mixing performance. This result may further be confirmed by the stable mixing time at location 3, which is similar to the result in Section 3.3.1.

3.3.3. Effects of fluid height in the storage tank

Circulating bulk-flow is a key factor influencing the mixing performance of the PJM because it influences the suspension time and transportation of particles. The gravity action that has to be conquered by the circulating bulk-flow increases with an increase in the fluid height in the tank, which results in a reduced circulating bulk-flow. To investigate the effects of the fluid height, a series of tests were performed under the following conditions: mass concentration of particles = 36.31%; initial height of the solid layer = 10 cm; liquid viscosity, $\mu = 1.21$ mPa·s; height of the mixing nozzle exit from the tank bottom, $H_b = 10$ cm; maximum-level setting in the ballast, $H_1 = 120$ cm; static pressure, $P_{c0} = 260$ kPa; and vent period, $t_1 = 10$ s. As shown in Fig. 19, the average mixing index η decreases with an increase in the fluid height in the tank.

3.3.4. Effects of maximum fluid level in the ballast

The fluid volume drawn during the suction phase is determined by the maximum fluid level in the ballast. A higher level produces a longer compression period. With an increase in the duration of the mixing jet flow, the energy available for mixing increases. Fig. 20 shows the experimental results, where the following conditions were employed: mass concentration of particles = 36.31%; initial height of

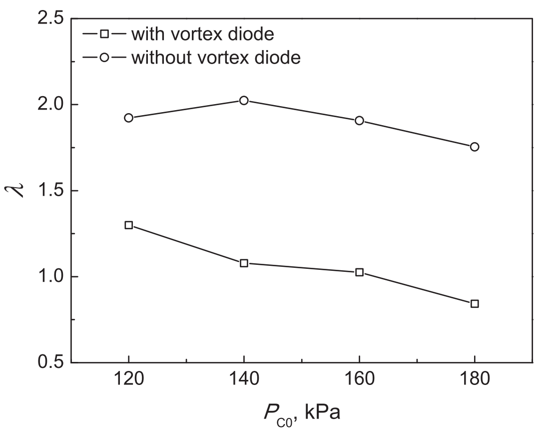

Fig. 12. Comparison of λ variation with static compression pressure (mixing nozzle B, d_1, 4 mm; d_2, 6 mm; D, 17.25 mm; H_b, 10 cm; H_l, 120 cm; H_v, 50 cm).

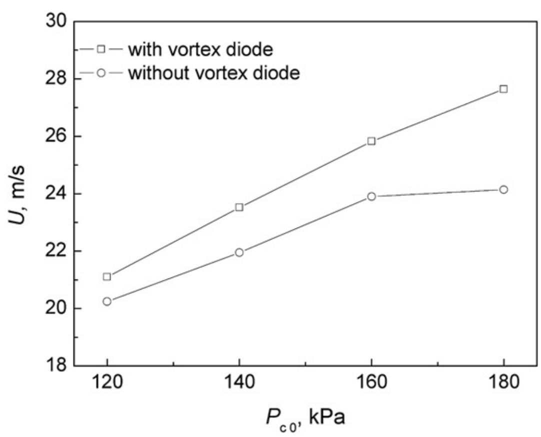

Fig. 13. Effects of vortex diode on mixing jet flow velocity (mixing nozzle B, d_1, 4 mm; d_2, 6 mm; D, 17.25 mm; H_b, 10 cm; H_l, 120 cm; H_v, 50 cm).

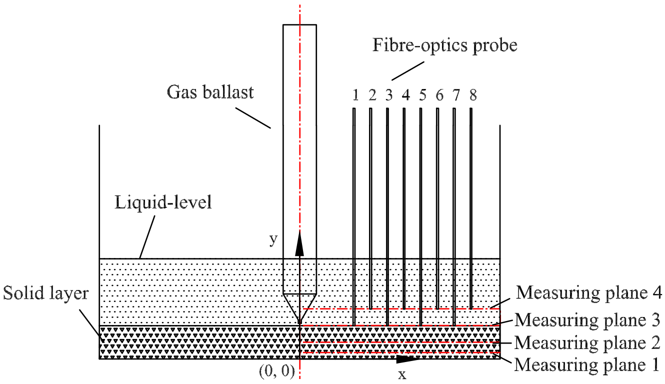

Fig. 14. Layout of fiber-optic probes in the storage tank.

the solid layer = 10 cm; liquid viscosity, μ = 1.21 mPa·s; height of the mixing nozzle exit from the tank bottom, H_b = 10 cm; height of the fluid level in the tank, H_v = 30 cm; static pressure, P_{c0} = 260 kPa; and vent period, t_1 = 10 s. An increase in the maximum fluid level of the ballast enhances the average mixing index η.

4. Conclusions

This study focused on the mixing processes for radioactive, corrosive, toxic, high-temperature, and/or high-solid-content hazardous liquid–solid mixtures. To ensure a maintenance-free feature, a maximum/minimum fluid level detection system without mechanical moving parts was proposed, which consisted of a Venturi tube, vortex diode, piezometric tube, and differential pressure meter. The proposed level detection system can effectively detect whether the maximum/minimum fluid level in the ballast is reached. To inhibit the leakage of compressed air during the compression phase, a vortex diode was inserted between the compression and suction injectors. This vortex diode was effective at inhibiting the leakage of compressed air. Moreover, a complete maintenance-free PJM was tested to evaluate the mixing performance for a liquid–solid mixture prepared using quartz sand and a water solution of glycerine. The maintenance-free PJM is promising to mix the hazardous mixtures, depending on the proposed level detection system and the method used to inhibit the leakage of compressed air. It could also be used for a liquid–solid mixture with a high liquid viscosity and particle concentration. The mixing performance of the maintenance-free PJM increased with increases in the static pressure of compressed air and the compression time, but decreased with increases in the liquid viscosity and fluid level in the storage tank.

Table 2
Location parameters of fiber-optics probes in storage tank.

Fiber-optics probe	1	2	3	4	5	6	7	8
x (cm)	17	22	27	32	37	42	47	52

Note: distances of measuring plane 1, 2, 3 and 4 are 2 cm, 5 cm, 10 cm and 15 cm respectively apart from tank bottom.

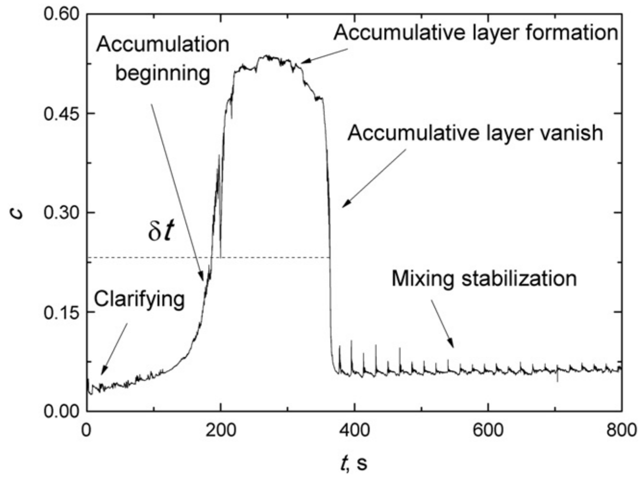

Fig. 16. Variation in solid concentration at location 3.

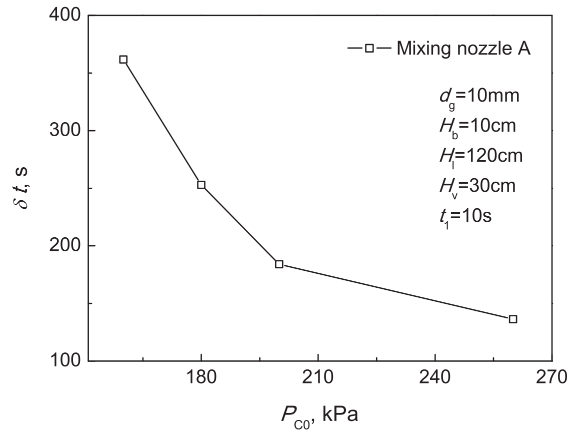

Fig. 17. Effects of static pressure of the compressed air on local stable mixing time.

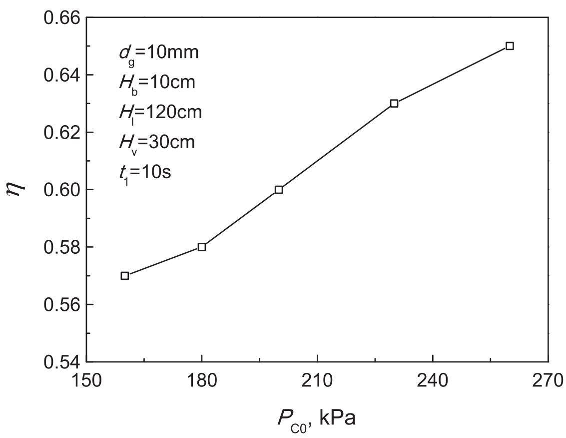

Fig. 15. Effects of static pressure of the compressed air on the average mixing index.

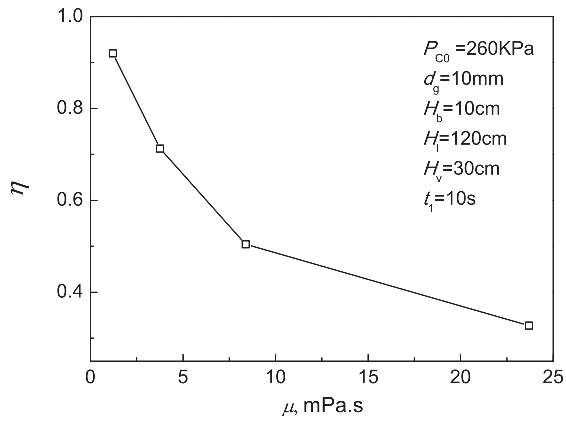

Fig. 18. Effects of liquid phase viscosity on the average mixing index.

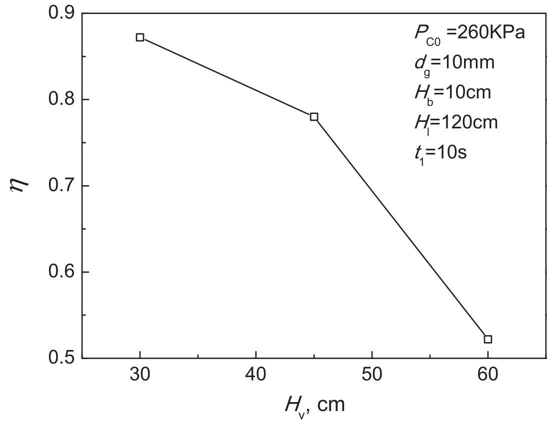

Fig. 19. Effects of fluid level in the storage tank on the average mixing index.

Notation

Symbols

c_{i0}	Initial bulk concentration of particle at location *i* in the storage tank, m^3/m^3
c_i	Bulk concentration of particle at location *i* in the storage tank at time *t*, m^3/m^3
$\overline{c}$	Uniform bulk concentration of particle averaged over the whole storage tank, m^3/m^3
D	Suction throat length in the suction injector and compression injector, mm
d_1	Nozzle exit diameter in the suction injector, mm
d_2	Nozzle exit diameter in the compression injector, mm
d_c	Quartz sank particle diameter, μm
d_g	Mixing nozzle exit diameter in the gas ballast, mm
$dP_{c,j}$	Pressure difference between the connection tube during the compression phase, kPa
$dP_{s,j}$	Pressure difference between the connection tube during the suction phase, kPa
dP_v	Pressure difference between upper and lower sides of the Venturi tube, kPa
H_a	Distance of the gas ballast axial line apart from the tank wall, cm
H_b	Distance of the mixing nozzle exit apart from the tank bottom, cm
H_l	Setting maximum fluid level in the gas ballast, cm
H_v	Fluid level in the storage tank, cm
n	Channel number of fiber-optic probes
P_{c0}	Static pressure of compressed gas, kPa
P_d	Pressure at gas ballast top, kPa
t	Time, s
t_v	Vent phase period, s
U	Jet flow velocity at mixing nozzle exit, m/s
V_l	Liquid volume in solid–liquid mixture, m^3
V_r	Particle size distribution percent of quartz sand particle
V_s	Quartz sand volume in solid–liquid mixture, m^3

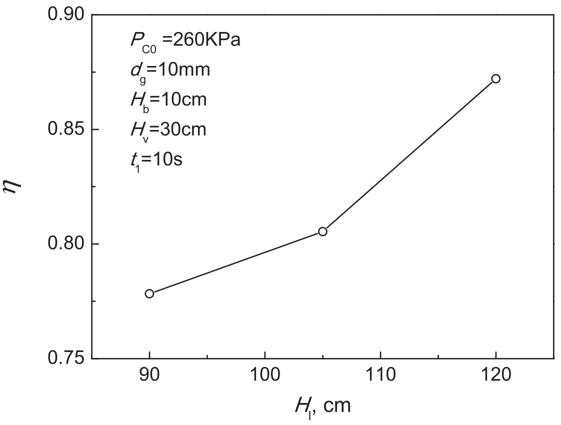

Fig. 20. Effects of maximum fluid level in the gas ballast on the average mixing index.

Greek letters

ρ_s	Quartz sand density, kg/m^3
μ	Liquid phase viscosity, mPa·s
λ	Dimensionless parameter to evaluate the extent of compressed air leakage
η	Mixing index averaged over volume framed by fiber-optic probes
δt	Stable mixing time at location 3, s.

References

[1] P.C. Luo, Y. Cheng, Z.W. Wang, Y. Jin, W.H. Yang, Research progress of liquid–liquid fast mixing equipment, Chemical Industry and Engineering Progress 24 (12) (2005) 1319–1326.
[2] P. Kalaichelvi, Y. Swarnalatha, T. Raja, Mixing time estimation and analysis in a jet mixer, ARPN Journal of Engineering and Applied Sciences 2 (5) (2007) 35–43.
[3] A.W. Patwardhan, S.G. Gaikwad, Mixing in tanks agitated by jets, Chemical Engineering Research and Design 81 (2) (2003) 211–220.
[4] A.W. Patwardhan, CFD modeling of jet mixed tanks, Chemical Engineering Science 57 (8) (2002) 1307–1318.
[5] A.W. Patwardhan, A.R. Thatte, Process design aspects of jet mixers, The Canadian Journal of Chemical Engineering 82 (2004) 198–205.
[6] H.D. Zughbi, M.A. Rakib, Mixing in a fluid jet agitated tank: effects of jet angle and elevation and number of jets, Chemical Engineering Science 59 (4) (2004) 829–842.
[7] H.D. Zughbi, I. Ahmad, Mixing in liquid-jet-agitated tanks: effects of jet asymmetry, Industrial and Engineering Chemistry Research 44 (2005) 1052–1066.
[8] P. Fallows, M. Williams, P. Murray, Applications of power fluidics technology in nuclear waste processing plants, In: WM'05 Conference, Tucson, AZ, 2005.
[9] B.E. Lewis, Extended Cold Testing of a Russian Pulsating Mixer Pump at the Oak Ridge National Laboratory, Oak Ridge, Tennessee, 2002.
[10] P.A. Meyer, D.E. Kurath, C.W. Stewart, Overview of the Pulse Jet Mixer Non-Newtonian Scaled Test Program, Richland, Washington, 2005.
[11] H.N. Guerrero, K.R. Eberl, Pulse jet mixing of a non-Newtonian waste slurry stimulant, In: Proceedings of 2005 ASME Fluids Engineering Division Summer Meeting, Houston, TX, USA, 2005, pp. 1846–1852.
[12] J.A. Bamberger, P.A. Meyer, Characterizing pulsating mixing of slurries, In: 2007 Proceedings of the 5th Joint ASME/JSME Fluids Engineering Summer Conference, San Diego, California USA, 2, 2007, pp. 201–206.
[13] B. Rosendall, W. Feng, C. Barringer, K.J. Knight, Validating CFD models of multiphase mixing in the waste treatment plant at the Hanford site, In: International Conference on Nuclear Engineering, Proceedings of ICONE, 14, 2006.

Associated professor Dr. Cong Xu

- 2004 to present: Works in the Institute of Nuclear and New Energy Technology, Tsinghua University. Field: Power fluidic technology and moving bed.
- 2002–2004: Worked in the Institute of Process Engineering, Chinese Academy of Sciences. Field: Fluidized bed.

Yi Huang

- September 2009 to present: MA candidate at Tsinghua University.
- Research topic: Experimental Study on the Fundamental Performance of Pulse Jet Mixer Used in the Nuclear Industry.